Article

Minimal Representations for Testing and Estimation in Projective Spaces

WOLFGANG FÖRSTNER, Bonn

Summary: Testing and estimation using homogeneous coordinates and matrices has to cope with obstacles such as singularities of covariance matrices and redundant parametrisations. The paper proposes a representation of the uncertainty of all types of geometric entities which (1) only requires the minimum number of parameters, (2) is free of singularities, (3) enables to exploit the simplicity of homogeneous coordinates to represent geometric constraints and (4) allows to handle geometric entities which are at infinity or at least very far away. We develop the concept, discuss its usefulness for bundle adjustment and demonstrate its applicability for determining 3D lines from observed image line segments in a multi view setup.

Zusammenfassung: Beim Testen und Schätzen mit homogenen Koordinaten und Matrizen treten wegen der Redundanz der Repräsentationen und der daraus folgenden Singularität der Kovarianzmatrizen Schwierigkeiten auf. Der Beitrag schlägt eine Repräsentation für die Unsicherheit geometrischer Elemente vor, die (1) eine minimale Zahl von Parametern benötigt, (2) frei von Singularitäten ist, (3) die Einfachheit homogener Koordinaten bei der Formulierung geometrischer Bedingungen belässt und (4) uneigentliche Elemente, d.h. Elemente im Unendlichen bzw. sehr weit entfernte Elemente behandeln kann. Wir stellen das Konzept vor, diskutieren seine Nützlichkeit bei der Bündelausgleichung und zeigen seine Anwendbarkeit für die Schätzung von 3D Geraden aus mehreren Bildern.

1 Introduction

Estimation of entities in projective spaces, such as points or transformations, has to cope with the *scale ambiguity* of the redundant representations of these entities, and, as a consequence, with the definition of *proper metrics* which results from the singularity of the covariance matrices. As an unwanted side effect the number of parameters heavily increases in large estimation problems. The paper shows how to consistently perform statistical testing and maximum likelihood (ML) estimation for geometric entities and transformations in projective spaces including elements at infinity while only handling the minimum of required parameters.

The *scale ambiguity* of homogeneous entities results from the redundant representation, where two elements, say 2D points, x and y or

two rotations $\mathcal{R}$ and $\mathcal{R}'$ are identical, in case their representations with homogeneous coordinates, here with $\mathbf{x}$ and $\mathbf{y}$ or with quaternions, here $\mathbf{q}$ and $\mathbf{q}'$, are proportional. This ambiguity regularly is avoided by proper normalization of the homogeneous entities. Mostly one applies either Euclidean normalization of homogeneous coordinates, say $\mathbf{x}^e = \mathbf{x}/x_3$, see KANATANI (1996), then accepting that no elements at infinity can be represented, or spherical normalization, say $\mathbf{x}^s = \mathbf{x}/|\mathbf{x}|$ or $\mathbf{q}^s = \mathbf{q}/|\mathbf{q}|$, then accepting that the parameters to be estimated sit on a non-linear manifold, here the unit spheres S^2 or S^3, see COLLINS (1993), HEUEL (2004). The sign ambiguity usually does not cause difficulties, as the homogeneous constraints used for reasoning are independent on the chosen sign.

The *uncertainty* of an observed geometric entity in many practical cases, can be repre-

sented sufficiently well by a Gaussian distribution $\mathcal{N}(\boldsymbol{\mu}_x, \Sigma_{xx})$. The distribution of derived entities, $\underline{\mathbf{y}} = \boldsymbol{f}(\underline{\mathbf{x}})$, resulting from a non-linear transformation can also be approximated by a Gaussian distribution, using Taylor expansion at the mean $\boldsymbol{\mu}_x$ and omitting higher order terms, possibly requiring truncation of the given distribution, see HARTLEY & ZISSERMAN (2000, App.3). The degree of approximation depends on the relative accuracy and has been shown to be negligible in many cases, see CRIMINISI (2001, p. 55).

The invariance of estimates w.r.t. the choice of the normalization of the estimated entities usually is achieved by minimizing a function in the Euclidean space of observations, in the context of bundle adjustment being the reprojection error, leading to the objective function $\Omega = \sum_i (\underline{\boldsymbol{x}}_i - \hat{\underline{\boldsymbol{x}}}_i)^{\mathsf{T}} \Sigma_{x_i x_i}^{-1} (\underline{\boldsymbol{x}}_i - \hat{\underline{\boldsymbol{x}}}_i)$. This at the same time is the Mahalanobis distance between the observed and estimated entities and can be used to evaluate whether the model fits the data. A similar reasoning is used when estimating transformations, such as rotations based on quaternions $\mathbf{q} = (q, \boldsymbol{q})$ or projective transformations, e.g. 2D homographies H, where one of the redundant elements, say the scalar part q or the last element H_{33}, is Euclideanly normalized to 1 in order to arrive at a minimal representation.

This situation becomes difficult, in case one wants to handle elements at infinity, thus homogeneous coordinate 3-vectors with $x_3 = 0$, rotations with $q \approx 0$, thus around 180°, or homographies with $H_{33} \approx 0$, and therefore one wants to use spherically normalized homogeneous vectors or matrices, or at least normalized direction vectors when using omnidirectional cameras, as their covariance matrices are or become close to singular.

Therefore, in case we want to use these normalized vectors or matrices as observed quantities, already the formulation of the objective function based on homogeneous entities is not possible and requires a careful discussion about estimable quantities (MEIDOW et al. 2009). Also the redundant representation requires additional constraints, which lead to Lagrangian parameters in the estimation process. As an example, one would need four parameters to estimate a 2D point, three for the homogeneous coordinates and one Lagrangian for the constraint, two parameters more than the degrees of freedom of a 2D point.

Related work

This problem of representing uncertain transformations has been addressed successfully for geometric transformations. Common to these approaches is to represent the uncertain transformations, say a rotation $\underline{R}$ as multiplicative deviations $R(\underline{r})$ from the mean transformation $\mathbb{E}(\underline{R})$ and to represent the small deviations as the exponential of a matrix, say $\exp(S(\underline{r}))$, which allows simple estimation and rigorous update, a property resulting from the group properties of these transformations. Based on the work of BREGLER & MALIK (1998), ROSENHAHN et al. (2002) used the exponential map for modelling spatial Euclidean motions, composed of rotations and translations in $\mathbb{R}^3$. BARTOLI & STURM (2004) used the idea to estimate the fundamental matrix with a minimal representation $\mathsf{F} = R_1 \, \mathrm{Diag}(\exp(\lambda), \exp(-\lambda), 0) \, R_2^{\mathsf{T}}$, twice using the rotation group and once the multiplication group $\mathbb{R}^+$. BEGELFOR & WERMAN (2005) showed how to estimate a general 2D homography with a minimal representation statistically rigorously, namely using the special linear group of 3×3-matrices with determinant 1, represented as $\mathsf{H} = \exp(K)$ with matrices K having trace zero, correctly reflecting the number of degrees of freedom, see the application in MEIDOW (2011).

To my knowledge the only attempts to use minimal representations for geometric entities other than transformations have been given by STURM & GARGALLO (2007) and ÅSTRÖM (1998), however, both are not able to represent elements at infinity, namely conics and points at infinity respectively.

This paper presents a concept for statistical testing and estimation with all types of geometric entities in projective spaces using minimal representations which are free of singularities and allow to handle entities at infinity (FÖRSTNER 2010 a,b).

Notation

We name objects with calligraphic letters, say a point χ. We denote Euclidean coordinates

with a slanted letter x, homogeneous coordinates with an upright letter **x**. Matrices are denoted with sans serif capital letters, say R, or upright in case of homogeneous matrices, e.g. H. The operator $N(\cdot)$ normalizes a vector to unit length. We adopt the Matlab syntax to denote the stack of two vectors or matrices, e.g. $z = [x; y] = [x^T, y^T]^T$. The vec-operator stacks the columns of a matrix to obtain a vector: $\text{vec}(A) = \text{vec}([a_1, …, a_n]) = [a_1; …; a_n]$. Stochastic variables are underscored, e.g. $\underline{x}$. We use the skew symmetric matrix $S(a)$ of a 3-vector, inducing the cross product $a \times b = S(a) b$. As an exception, we denote three-dimensional rotation vectors – the product of the rotation angle with the normalized rotation axis – with r and four dimensional quaternion vectors with **q**, instead with capital letters.

2 Minimal Representation of Uncertainty

The natural spaces of homogeneous entities are the unit spheres S^n, possibly constrained to a subspace. Spherically normalized homogeneous coordinates of 2D points (x^s) and lines (l^s) live on the sphere S^2 in $\mathbb{R}^3$, those of 3D points (X^s) and planes (A^s) on the 3-sphere S^3 in $\mathbb{R}^4$ respectively. Also unit quaternions, allowing to represent all rotations $\mathcal{R}$ without singularities, live on the unit sphere S^3. Lines in 3D, represented by Plücker coordinates (L^s), live on the so-called Klein quadric Q which is the subspace of the unit sphere S^5 in $\mathbb{R}^6$ restricted by the Plücker constraint. Planar homographies, represented by 3×3-matrices may be normalized either enforcing their Frobenius norm $\|H\|^2 = \sum_{ij} H_{ij}^2$ or their determinant $|H|$ to be 1, then their vector $h = \text{vec}(H)$ also live on a unit sphere, namely S^8 or in another non-linear space respectively. Other transformations, such as the singular correlation matrix E of the relative orientation, called essential matrix, can be represented by products of basic transformations, e. g. $E = S(b) R^T$, as a function of a homogeneous 3-vector, the base direction **b**, and the rotation R.

How to represent uncertain elements on these curved manifolds is the topic of the next section.

2.1 Representation of Uncertainty in non-linear Subspaces

The principle of testing and estimation of entities can be easily visualized, if they live on a one-dimensional manifold in 2D, see Fig. 1. In both cases we assume the uncertainty of the entities is small enough compared to the curvature of the manifold to represent it as a covariance matrix in the tangent space. The approximate value may deviate from the mean value. In order to realize this procedure we need to define (1) the tangent space, which is used for representing the uncertainty and performing the testing and the estimation, and (2) the forward and (3) the backward projection taking the uncertainty of the entities into account. The definition of the tangent space in all cases is realized by linearisation, while the forward and backward projections differ for transformations and geometric entities: While the manifolds of transformations are represented explicitly, the manifolds for geometric entities are represented implicitly, requiring special care.
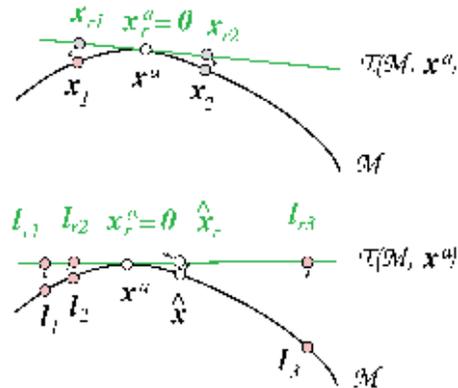

Fig. 1: Above: Testing the identity of two points x_1 and x_2: the points are first projected into the tangent space $\mathcal{T}(\mathcal{M}, x^a)$ of the manifold $\mathcal{M}$ at some approximate value x^a, leading to a substitute test of x_{r1} and x_{r2}. Below: Estimating the mean of three observations $l_i, i = 1, 2, 3$ is performed in the tangent space $\mathcal{T}(\mathcal{M}, x^a)$ at the approximate value x^a after projecting them to l_{ri} leading to an updated estimate $\hat{x}_r$ and, after back projecting to the manifold, to the estimate $\hat{x}$.

2.2 *Minimal Representation for Uncertain Transformations*

We explain the principle of representing uncertain transformations using rotations in 3D.

Uncertain rotations

Take the space S^3 of rotations, represented by rotation matrices $R \in \mathbb{R}^{3\times 3}$. Starting from the mean rotation $\mathbb{E}(R)$ a neighbouring uncertain rotation $\underline{R}$ can be represented by

$$\underline{R} = R(\underline{r}) \ \mathbb{E}(R), \tag{1}$$

where $R(\underline{r})$ represents a small rotation, close to the unit matrix depending on the stochastic 3-vector $\underline{r}$. Its 3×3-covariance matrix Σ_{rr} minimally and uniquely represents the uncertainty of the rotation matrix $\underline{R}$. Obviously, the vector r lies in the three-dimensional tangent space $\mathbb{R}^3$ of the rotations, evaluated at the zero-rotation $\mathcal{R}(\mathbf{0})$, represented by the unit matrix I_3. The function

$$R(r) = \exp\big(S(r)\big) \tag{2}$$

$$= I_3 + S(r) + \frac{1}{2!}S^2(r) + \dots$$

$$= I_3 + \frac{\sin(|r|)}{|r|}S(r) + \frac{1-\cos(|r|)}{|r|^2}S^2(r)$$

maps the three-dimensional linear tangent space $\mathbb{R}^3$ to the spherical space S^3 of rotations. The transition from the second to the third line of (2), uses the easy to be proved fact: $S^3(r) = -|r|^2 S(r)$ for collecting higher order terms of $S(r)$, see HARTLEY & ZISSERMAN (2000, A4.9). This function is called the exponential map. In general, the exponential of a skew symmetric matrix is a rotation matrix. The exponential map can only represent rotations with angles $\neq \pm 180°$, which is no restriction in our context.

The mapping from a rotation R to the tangent space at an approximate rotation can easily be achieved from the linearised version of (1) using some approximate rotation R^a being some estimate for the mean rotation, thus

$$R \approx (I_3 + S(r))R^a \quad \text{or} \quad S(r) \approx RR^{a\top} - I_3 \tag{3}$$

yielding $r = [S_{23}; S_{31}; S_{12}]$. As the elements of r occur linearly in (3), left, it also is used for linearisation within an estimation procedure.

The non-linear manifold, here of rotations, obviously can be *explicitly* represented, here by using the exponential map (2), which in the context of estimation using the Gauß-Markov model, is just a special case of a non-linear function of the unknown parameters.

Uncertain homographies

This principle of representing an uncertain transfomation can be generalized to uncertain 2D or 3D homographies and their specialisations, namely 2D and 3D motions and similarities. An uncertain 2D homography, for example, can be represented as a left-product of the mean homography $\mathbb{E}(H)$ and a small uncertain homography $H(\underline{k})$

$$\underline{H} = H(\underline{k}) \ \mathbb{E}(H). \tag{4}$$

The small homography is close to the unity, as can be seen, when analysing the linearisation of the transformation of the Cartesian coordinates. It depends on a stochastic 8-vector $\underline{k}$. We assume the matrices to have determinant one, thus being spectrally normalized $|H| = \prod_i \lambda_i = 1$, using the eigenvalues λ_i of H. Homographies close to the unit matrix having determinant one can again be represented by the exponential map

$$H(k) = \exp\big(K(k)\big) = I_3 + K(k) + \frac{1}{2!}K^2(k) + \dots \tag{5}$$

with the zero-trace matrix

$$K(k) = \begin{bmatrix} k_1 & k_4 & k_7 \\ k_2 & k_5 & k_8 \\ k_3 & k_6 & -k_1-k_5 \end{bmatrix}. \tag{6}$$

Again the 8×8-covariance matrix Σ_{kk} minimally and uniquely, up to the convention of the trace-less matrix K (BEGELFOR & WERMAN 2005), represents the uncertainty of the spectrally normalized homography $\underline{H}$. Linearisation of (4) at a given approximate homography H^a therefore leads to

$$\mathsf{H} \approx (I_3 + K(\boldsymbol{k}))\,\mathsf{H}^a, \tag{7}$$

which can be used within an iterative estimation procedure and allows to determine $\boldsymbol{k}$ for a homography H close to an approximate one H^a, taking the first eight values of $\mathrm{vec}\,(\mathsf{H}\,(\mathsf{H}^a)^{-1} - I_3)$.

Finally, it might be useful for some applications to represent both, the homography and its inverse, linearly in 8 parameters, which can easily be achieved using $\underline{\mathsf{H}}^{-1} = (\mathbb{IE}(\mathsf{H})^{-1}\,\mathsf{H}\,(-\underline{\boldsymbol{k}}))$ $\approx (\mathbb{IE}(\mathsf{H}))^{-1}\,(I_3 - K(\underline{\boldsymbol{k}}))$ together with (4).

2.3 *Minimal Representation for Uncertain Points in 2D and 3D*

We will now transfer the concept to uncertain unit vectors on the unit sphere S^2, representing 2D points and lines, and generalize it to other geometric entities.

Let an uncertain 2D point χ be represented with its mean, the 2-vector $\boldsymbol{\mu}_x$ and its 2×2-covariance matrix Σ_{xx}. It can be visualized by the standard ellipse $(\boldsymbol{x} - \boldsymbol{\mu}_x)^\mathsf{T} \Sigma_{xx}^{-1} (\boldsymbol{x} - \boldsymbol{\mu}_x) = 1$. Spherically normalizing the homogeneous vector $\mathbf{x} = [\boldsymbol{x}; 1] = [u, v, w]^\mathsf{T}$ yields

$$\mathbf{x}^s = \frac{\mathbf{x}}{|\mathbf{x}|}, \quad \Sigma_{\mathbf{x}^s \mathbf{x}^s} = J \Sigma_{\mathbf{x}\mathbf{x}} J^\mathsf{T} \tag{8}$$

with the 3×3-matrix

$$\Sigma_{\mathbf{x}\mathbf{x}} = \begin{bmatrix} \Sigma_{xx} & \mathbf{0} \\ \mathbf{0}^\mathsf{T} & 0 \end{bmatrix} \tag{9}$$

using the Jacobian

$$J = \frac{\partial \mathbf{x}^s}{\partial \mathbf{x}} = \frac{1}{|\mathbf{x}|}(I_3 - \mathbf{x}^s \mathbf{x}^{s\mathsf{T}}) \tag{10}$$

with $\mathrm{rank}\,(\Sigma_{\mathbf{x}\mathbf{x}}) = 2$ and $\mathrm{null}\,(\Sigma_{\mathbf{x}\mathbf{x}}) = \boldsymbol{\mu}_x^s$. As the smallest eigenvalue is zero, the standard ellipsoid is flat and lies in the tangent space of $\mathbf{x}$ at S^2.

In the following we assume all point vectors $\mathbf{x}$ to be spherically normalized and omit the superscript ^{s} for simplicity of notation.

We now want to choose a coordinate system $[\boldsymbol{s}, \boldsymbol{t}]$ in the tangent space $\perp \boldsymbol{\mu}_x$, and represent the uncertainty by a 2×2-matrix in that coordinate system (Fig. 2).
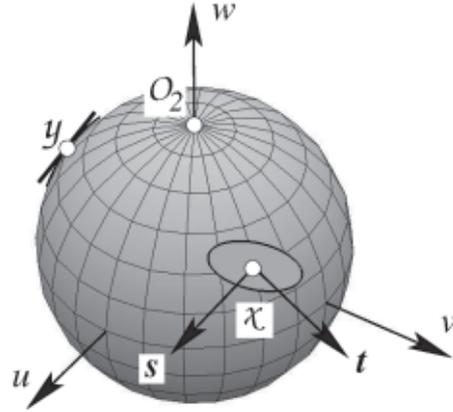
Fig. 2: Minimal representation for an uncertain point $\chi(\underline{\mathbf{x}})$ on the unit sphere S^2 representing the projective plane $\mathbb{IP}^2$ by a flat ellipsoid in the tangent plane at the mean $\boldsymbol{\mu}_x$. The uncertainty has only two degrees of freedom in the tangent space spanned by two basis vectors $\boldsymbol{s}$ and $\boldsymbol{t}$ of the tangent space, being the null space of $\boldsymbol{\mu}_x^\mathsf{T}$. The uncertainty should not be too large, such that the deviation of the distribution on the sphere and on the tangent plane do not differ too much, as at point y.

This is easily achieved by using the orthonormal matrix collecting the two base vectors $\boldsymbol{s}$ and $\boldsymbol{t}$.

$$J_r(\boldsymbol{\mu}_x) = \mathrm{null}(\boldsymbol{\mu}_x^\mathsf{T}) = [\boldsymbol{s}, \boldsymbol{t}], \quad [\boldsymbol{\mu}_x^\mathsf{T}\boldsymbol{s}, \boldsymbol{\mu}_x^\mathsf{T}\boldsymbol{t}] = \mathbf{0}^\mathsf{T},$$

$$\tag{11}$$

fulfilling $J_r^\mathsf{T}(\boldsymbol{\mu}_x)\,J_r(\boldsymbol{\mu}_x) = I_2$. The subscript r in J_r stands for the reduced (tangent) space.

The normal of the tangent space is $\boldsymbol{\mu}_x$. This results from linearising the constraint $h = \underline{\mathbf{x}}^\mathsf{T}\underline{\mathbf{x}} - 1 = 0$ w.r.t. $\underline{\mathbf{x}}$ leading to the linear constraint $\boldsymbol{\mu}_x^\mathsf{T}\Delta\underline{\mathbf{x}} = 0$, expressing the fact, that any deviation of a vector from the mean $\boldsymbol{\mu}_x$ is perpendicular to $\boldsymbol{\mu}_x$.

We now represent the stochastic 2-vector $\underline{\boldsymbol{x}}_r$ with mean $\boldsymbol{\mu}_{x_r} = 0$ and covariance $\Sigma_{x_r x_r}$ in the tangent space at $\boldsymbol{\mu}_x$. In order to arrive at a spherically normalized random vector $\underline{\mathbf{x}}$ with mean $\boldsymbol{\mu}_x$ we need to spherically normalize the vector $\underline{\mathbf{x}}^t = \boldsymbol{\mu}_x + J_r(\boldsymbol{\mu}_x)\boldsymbol{x}_r = \boldsymbol{\mu}_x + \underline{x}_{r,1}\,\boldsymbol{s} + \underline{x}_{r,2}\,\boldsymbol{t}$ in the tangent space and obtain

$$\underline{\mathbf{x}}(\boldsymbol{\mu}_x, \underline{\boldsymbol{x}}_r) = \mathsf{N}(\boldsymbol{\mu}_x + J_r(\boldsymbol{\mu}_x)\,\underline{\boldsymbol{x}}_r) \tag{12}$$

$$J_r(\mathbf{\mu}_x) = \left.\frac{\partial \mathbf{x}}{\partial \mathbf{x}_r}\right|_{x=\mu_x}. \tag{13}$$

We thus can identify $J_r(\mathbf{\mu}_x)$ with the Jacobian of this transformation evaluated at $\mathbf{x} = \mathbf{\mu}_x$. The inverse transformation is the reduction of the homogeneous vector to its reduced counterpart

$$\underline{x}_r^\tau = J_r^\top(\mathbf{\mu}_x)\underline{\mathbf{x}}. \tag{14}$$

omitting the superscript τ in case no confusion is to be expected. Since $J_r^\top(\mathbf{\mu}_x)\mathbf{\mu}_x = \mathbf{0}$ the mean of $\underline{x}_r$ is the zero vector, $\mathbf{\mu}_{x_r} = \mathbf{0}$, as specified.

This allows to establish the one-to-one correspondence between the *reduced covariance matrix* $\Sigma_{x_r x_r}$ of the reduced coordinates $\underline{x}_r$ and the covariance matrix Σ_{xx} of $\underline{\mathbf{x}}$:

$$\Sigma_{xx} = J_r(\mathbf{\mu}_x)\Sigma_{x_r x_r}J_r^\top(\mathbf{\mu}_x) \tag{15}$$

$$\Sigma_{x_r x_r} = J_r^\top(\mathbf{\mu}_x)\Sigma_{xx}J_r(\mathbf{\mu}_x). \tag{16}$$

We use (14) to derive *reduced* observations and parameters and after estimating corrections $\widehat{\Delta x}_r$ then apply (12) to find corrected estimates $\hat{\mathbf{x}} = \hat{\mathbf{x}}(\mathbf{x}^a, \widehat{\Delta x}_r)$.

The non-linear manifold, here of the 3-vectors of homogeneous coordinates, is *implicitly* represented, here by the unit norm constraint, just as in estimation models using constraints onto the observations or the unknown parameters.

A similar reasoning leads to the representation of 3D points. Again, the Jacobian, $J_r(\mathbf{\mu}_X)$ overloading the function $J_r(\cdot)$, is the null space of $\mathbf{X}^\top$ and spans the three-dimensional tangent space of S^3 at $\mathbf{\mu}_X$. The relations between the singular 4×4-covariance matrix of the spherically normalized vector $\mathbf{X}$ and the reduced 3×3-covariance matrix $\Sigma_{X_r X_r}$ are equivalent to (15) and (16).

Homogeneous 3-vectors $\mathbf{l}$ representing 2D lines and homogeneous 4-vectors $\mathbf{A}$ representing planes can be handled in the same way.

2.4 *Minimal Representation for Straight 3D Lines*

We now generalize the concept for 3D lines. Lines $\mathcal{L}$ in 3D are represented by their normalized Plücker coordinates $\mathbf{L} = [\mathbf{L}_h; \mathbf{L}_0] = \mathsf{N}([\mathbf{Y}-\mathbf{X}, \mathbf{X}\times\mathbf{Y}])$ in case they are derived by joining two points $\mathcal{X}(\mathbf{X})$ and $\mathcal{Y}(\mathbf{Y})$. Line vectors need to fulfill the quadratic Plücker constraint $\mathbf{L}_h^\top \mathbf{L}_0 = 0$ and span the Klein quadric Q consisting of all homogeneous 6-vectors fulfilling the Plücker constraint. The dual line $\bar{\mathcal{L}}(\bar{\mathbf{L}})$ has Plücker coordinates $\bar{\mathbf{L}} = [\mathbf{L}_0; \mathbf{L}_h]$, exchanging its first and second 3-vector. As in addition a 6-vector needs to fulfill the Plücker constraint in order to represent a 3D line, the space of 3D lines is four-dimensional.

The transfer of the minimal representation of points to 3D lines requires some care. The four-dimensional tangent space is perpendicular to $\mathbf{L}$, as $\mathbf{L}^\top\mathbf{L} - 1 = 0$ holds and perpendicular to $\bar{\mathbf{L}}$, as $\bar{\mathbf{L}}^\top\mathbf{L} = 0$ holds. Therefore, the tangent space is given by the four columns of the 6×4 matrix

$$J_r(\mathbf{L}) = \mathrm{null}\left(\left[\mathbf{L}, \bar{\mathbf{L}}\right]^\top\right) \tag{17}$$

again assuming this matrix to be orthonormal. Therefore for random perturbations $\underline{L}_r$ we have the general 6-vector

$$\underline{\mathbf{L}}^\tau(\mathbf{\mu}_L, \underline{L}_r) = \mathbf{\mu}_L + J_r(\mathbf{\mu}_L)\underline{L}_r \tag{18}$$

in the tangent space. In order to arrive at a random 6-vector, which is both spherically normalized and fulfills the Plücker constraint also for finite random perturbations we need to normalize $\mathbf{L}^\tau = [\mathbf{L}_h^\tau; \mathbf{L}_0^\tau]$ accordingly. The two 3-vectors $\mathbf{L}_h^\tau$ and $\mathbf{L}_0^\tau$ in general are not orthogonal. Following the idea of Bartoli & Sturm (2005) we therefore rotate these vectors in their common plane such that they become orthogonal. We use a simplified modification, as the normalization within an iteration sequence will have decreasing effect. We use linear interpolation of the directions $\mathbf{D}_h^\tau = \mathsf{N}(\mathbf{L}_h^\tau)$ and $\mathbf{D}_0^\tau = \mathsf{N}(\mathbf{L}_0^\tau)$ (Fig. 3). With the distance $d = |\mathbf{D}_h^\tau - \mathbf{D}_0^\tau|$ and the shortest distance $r = \sqrt{1 - d^2/4}$ of the origin to the line joining $\mathbf{D}_h^\tau$ and $\mathbf{D}_0^\tau$ we have

Fig. 3: Enforcing the Plücker constraint onto a 6-vector $\mathbf{L}^\tau = [\boldsymbol{L}_h^\tau; \boldsymbol{L}_0^\tau]$. Starting from vectors $\boldsymbol{D}_h^\tau = \mathsf{N}(\boldsymbol{L}_h^\tau)$ and $\boldsymbol{D}_0^\tau = \mathsf{N}(\boldsymbol{L}_0^\tau)$, which in general are not perpendicular, we easily can enforce the perpendicularity by symmetric linear interpolation, leading to $\boldsymbol{D}_h$ and $\boldsymbol{D}_0$, which are perpendicular. The vector $\mathbf{M} = \mathsf{N}([|\boldsymbol{L}_h|\boldsymbol{D}_h; |\boldsymbol{L}_0|\boldsymbol{D}_0])$ yields a valid Plücker vector close to $\mathbf{L}^\tau$.

$$\boldsymbol{D}_{h,0} = (1/2 \pm r/d)\boldsymbol{D}_h^\tau + (1/2 \mp r/d)\boldsymbol{D}_0^\tau. \tag{19}$$

The 6-vector $\mathbf{M} = [|\boldsymbol{L}_h|\boldsymbol{D}_h; |\boldsymbol{L}_0|\boldsymbol{D}_0]$ now fulfills the Plücker constraint and preserves the length ratio of its two parts, as the vectors $\boldsymbol{D}_h$ and $\boldsymbol{D}_0$ have the same length by construction. The vector $\mathbf{M}$ finally needs to be spherically normalized. This leads to the normalized stochastic 3D line coordinates

$$\underline{\mathbf{L}} = \mathsf{N}(\underline{\mathbf{L}}^\tau(\boldsymbol{\mu}_\mathrm{L}, \underline{\boldsymbol{L}}_r)) \doteq \underline{\mathbf{M}}/|\underline{\mathbf{M}}| \tag{20}$$

which guarantees $\underline{\mathbf{L}}$ to sit on the Klein quadric, thus to fulfill the Plücker constraint.

The inverse relation to (20) is

$$\underline{\boldsymbol{L}}_r = J_r^\mathsf{T}(\boldsymbol{\mu}_\mathrm{L})\,\underline{\mathbf{L}} \tag{21}$$

as $J_r(\boldsymbol{\mu}_\mathrm{L})$ is an orthonormal matrix. The relations between the covariances of $\mathbf{L}$ and L_r therefore are

$$\boldsymbol{\Sigma}_\mathrm{LL} = J_r(\boldsymbol{\mu}_\mathrm{L})\boldsymbol{\Sigma}_{L_r L_r}J_r^\mathsf{T}(\boldsymbol{\mu}_\mathrm{L}) \tag{22}$$

$$\boldsymbol{\Sigma}_{L_r L_r} = J_r^\mathsf{T}(\boldsymbol{\mu}_\mathrm{L})\boldsymbol{\Sigma}_\mathrm{LL}\,J_r(\boldsymbol{\mu}_\mathrm{L}). \tag{23}$$

3 Estimation and Testing with minimal Representations

3.1 *Estimation*

Using the minimal representations introduced in the last section, we are able to perform ML estimation for all entities. We restrict the following discussion to the model containing constraints between observed and unknown entities only, known as Gauß-Helmert model. Generalizations to include constraints between the parameters only are possible. We start the derivation with the model where the observations have regular covariance matrices and then reduce the model, such that also observations with singular covariance matrices can be handled.

The optimization problem

We want to solve the following optimization problem

$$\text{minimize} \quad \Omega(\tilde{\boldsymbol{v}}) = \tilde{\boldsymbol{v}}^\mathsf{T}\boldsymbol{\Sigma}_{ll}^{-1}\,\tilde{\boldsymbol{v}} \tag{24}$$

$$\text{subject to} \quad \boldsymbol{g}(\boldsymbol{l} + \tilde{\boldsymbol{v}}, \tilde{\boldsymbol{x}}) = \mathbf{0} \tag{25}$$

where the N observations $\boldsymbol{l}$, their $N \times N$ covariance matrix $\boldsymbol{\Sigma}_{ll}$ and the G constraint functions $\boldsymbol{g}$ are given, and the N true corrections $\tilde{\boldsymbol{v}}$ to the observations and the U true parameters $\tilde{\boldsymbol{x}}$ are unknown. The number G of constraints needs to be larger than the number of parameters U. Also it is assumed that the constraints are functionally independent. The solution yields the ML estimates, namely the fitted observations $\hat{\boldsymbol{l}} = \boldsymbol{l} + \hat{\boldsymbol{v}}$ via $\hat{\boldsymbol{v}}$ and parameters $\hat{\boldsymbol{x}}$, under the assumption that the observations are normally distributed with covariance matrix $\boldsymbol{\Sigma}_{ll} = D(\underline{\boldsymbol{l}}) = D(\underline{\boldsymbol{v}})$, and the true observations $\tilde{\boldsymbol{l}}$ fulfill the constraints given the true parameters $\tilde{\boldsymbol{x}}$.

Example: Bundle adjustment

Bundle adjustment is based on the projection relation $\mathbb{E}(\mathbf{x}_{ij}') = \lambda_{ij} \mathsf{P}_j \mathbf{X}_i$ between the scene points $\mathcal{X}_i$, the projection matrices P_j and the image points $\mathbf{x}_{ij}$ of point $\mathbf{X}_i$ observed in camera j. The classical approach eliminates the indi-

vidual scale factors λ_{ij} by using Euclidean coordinates for the image points. Also the scene points are represented by Euclidean coordinates. This does not allow for scene or image points at infinity. This may occur when using omnidirectional cameras, where a representation of the image points in a projection plane is not possible for all points or in case scene points are very far away compared to the length of the motion path of a camera, e.g. at the horizon. There are two ways to eliminate the scale factor while being able to handle points at infinity.

1. The easiest way is to rewrite the model using spherical normalisation: $\mathbb{E}(\mathbf{x}_{ij}^{\prime s}) = \mathsf{N}(\mathsf{P}_j\,\mathbf{X}_i)$ and then multiplying each equation with $J_x(\mathbf{x}_{ij}^{\prime a\mathsf{T}})$ leading to $\mathbf{x}_{r,ij}^{\prime} = J_x(\mathbf{x}_{ij}^{\prime a\mathsf{T}})\,\mathsf{N}(\mathsf{P}_j\,\mathbf{X}_i)$. The reduced coordinates $\mathbf{x}_{r,ij}^{\prime}$ of the camera rays $\mathbf{x}_{r,ij}^{\prime s}$ have a regular covariance matrix, allowing to use the classical Gauß-Markov model for estimation.

2. The scale factor also can be eliminated by expressing the collinearity as $\mathbb{E}(\mathbf{x}_{ij}^{\prime}) \times \mathsf{P}_j\,\mathbf{X}_i = \mathbf{0}$, thus requiring the two homogeneous coordinate vectors $\mathbf{x}_{ij}^{\prime}$ and $\mathsf{P}_j\,\mathbf{X}_i$ to be parallel. These constraints between observations and unknown parameters thus require to use the Gauß-Helmert model from (24) (SCHNEIDER et al. 2011). However, we also can handle constraints of image lines $l_{ij}^{\prime}$ passing though the projected point $\mathsf{P}_j\,\mathbf{X}_i$, reading as $\mathbb{E}(\mathbf{l}_{ij}^{\prime\mathsf{T}})\,\mathsf{P}_j\,\mathbf{X}_i = 0$. Thus both types of constraints can be represented using (25).

The singularity of the covariance matrix of the spherically normalized image points and the necessity to represent the scene points also with spherically normalized homogeneous vectors, requires to use the corresponding reduced coordinates.

For solving the generally non-linear problem, we assume approximate values $\hat{\mathbf{x}}^a$ and $\hat{\mathbf{l}}^a$ for the fitted parameters and observations to be available. We thus search for corrections $\widehat{\Delta l}$ and $\widehat{\Delta x}$ for the fitted observations and parameters using $\hat{\mathbf{l}} = \mathbf{l} + \hat{\mathbf{v}} = \hat{\mathbf{l}}^a + \widehat{\Delta l}$ and $\hat{\mathbf{x}} = \hat{\mathbf{x}}^a + \widehat{\Delta x}$. With these assumptions we can rephrase the optimization problem: minimize $\Omega\,(\widehat{\Delta l})$ = $(\hat{\mathbf{l}}^a - \mathbf{l} + \widehat{\Delta l})^{\mathsf{T}}\,\Sigma_{ll}^{-1}\,(\hat{\mathbf{l}}^a - \mathbf{l} + \widehat{\Delta l})$ subject to $g\,(\hat{\mathbf{l}}^a + \widehat{\Delta l}, \hat{\mathbf{x}}^a + \widehat{\Delta x}) = \mathbf{0}$. The approximate values are iteratively improved by finding best estimates for $\widehat{\Delta l}$ and $\widehat{\Delta x}$ using the linearized constraints

$$g\,(\hat{\mathbf{l}}^a, \hat{\mathbf{x}}^a) + A\widehat{\Delta x} + B^{\mathsf{T}}\,\widehat{\Delta l} = \mathbf{0} \qquad (26)$$

with the corresponding Jacobians A and B of g to be evaluated at the approximate values.

Reducing the model

We now want to transform the model in order to allow for observations with singular covariances. For simplicity we assume the vectors $\mathbf{l}$ and $\mathbf{x}$ of all observations and unknown parameters can be partitioned into I and J individual and mutually uncorrelated observational vectors $\mathbf{l}_i$, $i = 1, \ldots, I$ and parameter vectors $\mathbf{x}_j$, $j = 1, \ldots, J$, referring to points, lines, planes, or transformations.

We first introduce the reduced observations $\mathbf{l}_{ri}$, the reduced corrections of the observations $\widehat{\Delta l}_{ri}$, and the reduced corrections $\widehat{\Delta x}_{rj}$:

$$\mathbf{l}_{ri} = J_r^{\mathsf{T}}(\hat{\mathbf{l}}_i^a)\,\mathbf{l}_i, \qquad (27)$$

$$\widehat{\Delta l}_{ri} = J_r^{\mathsf{T}}(\hat{\mathbf{l}}_i^a)\widehat{\Delta l}_i, \qquad (28)$$

$$\widehat{\Delta x}_{rj} = J_r^{\mathsf{T}}(\hat{x}_j^a)\widehat{\Delta x}_j, \qquad (29)$$

where each Jacobian refers to the type of the entity it is applied to. The reduced approximate values are zero, as they are used to define the reduction, e.g. from (14) we conclude for 2D points $\hat{\mathbf{x}}_r^a = J_r^{\mathsf{T}}(\hat{\mathbf{x}}^a)\,\hat{\mathbf{x}}^a = \mathbf{0}$. We collect the Jacobians in two block diagonal matrices $J_l^{\mathsf{T}} = \{J_r^{\mathsf{T}}(\hat{\mathbf{l}}_i^a)\}$ and $J_x^{\mathsf{T}} = \{J_r^{\mathsf{T}}(\hat{\mathbf{x}}_j^a)\}$ in order to arrive at the reduced observations $\mathbf{l}_r = J_l^{\mathsf{T}}\,\mathbf{l}$, the corrections for the reduced observations $\widehat{\Delta l}_r = J_l^{\mathsf{T}}\widehat{\Delta l}$ and parameters $\widehat{\Delta x}_r = J_x^{\mathsf{T}}\widehat{\Delta x}$.

Second we need to reduce the covariance matrices $\Sigma_{l_i l_i}$. This requires some care: As a covariance matrix is the mean squared deviation from the mean, we need to refer to the best estimate of the mean when using it. In our context the best estimate for the mean at the current iteration is the approximate value $\hat{\mathbf{l}}_i^a$. Therefore we need to apply two steps: (1) transfer the given covariance matrix, referring to $\mathbf{l}_i$, such that it refers to $\hat{\mathbf{l}}_i^a$ and (2) reduce the covariance matrix to the minimal representation $\hat{\mathbf{l}}_{ri}$. As an example, let the observations be 2D lines with spherically normalized homogeneous vectors $\mathbf{l}_i$. Then the re-

duction is achieved by: $\Sigma_{l_i^a l_i^a}^a = J_i^a \Sigma_{l_i l_i} J_i^{aT}$ with $J_i^a = J_r^T(l_i^a) R(l_i, \hat{l}_i^a)$ namely by first applying a minimal rotation from l_i to $\hat{l}_i^a$ (McGLONE et al. 2004), second reducing the covariance matrix following (15). The superscript ^{a} in $\Sigma_{l_i^a l_i^a}^a$ indicates the covariance to depend on the approximate values.

The reduced constraints now read as

$$g(\hat{l}^a, \hat{x}^a) + A_r \widehat{\Delta x}_r + B_r^T \widehat{\Delta l}_r = \mathbf{0} \qquad (30)$$

with

$$A_r = A J_x^T \quad B_r^T = B^T J_l^T. \qquad (31)$$

Now we need to minimize the weighted sum of the squared reduced corrections $\hat{v}_r = \hat{l}_r^a - l_r + \widehat{\Delta l}_r = -l_r + \widehat{\Delta l}_r$. Thus we need to minimize $\Omega(\widehat{\Delta l}_r) = (-l_r + \widehat{\Delta l}_r)^T (\Sigma_{l_r l_r}^a)^{-1} (-l_r + \widehat{\Delta l}_r)$ subject to the reduced constraints in (30).

The estimated corrections $\widehat{\Delta x}_r$ and $\widehat{\Delta l}_r$ to the reduced parameters and observations of the reduced linearised model are obtained from McGLONE et al. (2004, Tab. 2.3). They are used to update the approximate values for the parameters and the fitted observations using the corresponding non-linear transformations, e.g. for an observed 2D point one uses (12), for an unknown 3D line (20). Using (15) and (22), for example, one can determine the covariance matrices of the non-reduced homogeneous coordinate vectors.

3.2 *Testing the Identity of Two Entities*

Testing geometric relations using homogeneous coordinates in most cases leads to constraints which are linear in the coordinates of each geometric entity. Examples are the incidence of a 2D point χ and a 2D line l, namely the constraint $\mathbf{x}^T \mathbf{l} = 0$, of a 3D line $\mathcal{L}$ and a plane $\mathcal{A}$, namely the constraint $\Gamma(\mathbf{L})\mathbf{A} = \mathbf{0}$ with the Plücker matrix $\Gamma(\mathbf{L}) = \mathbf{X}\mathbf{Y}^T - \mathbf{Y}\mathbf{X}^T$ for a line $\mathcal{L}$ through the points $\mathcal{X}$ and $\mathcal{Y}$, or the identity of two points χ and y, namely the constraint $\mathsf{S}(\mathbf{x})\mathbf{y} = \mathbf{0}$. Among all these tests, the tests on the identity of two homogeneous entities can be simplified using reduced coordinates.

Let the two entities be two lines $\mathcal{L}_i(\mathbf{L}_i, \Sigma_{\mathbf{L}_i \mathbf{L}_i})$, $i = 1, 2$, specified by their, not necessarily normalized, Plücker coordinates and their covariance matrices. Testing their identity would require to test $\mu_{\mathbf{L}_1} = \lambda \mu_{\mathbf{L}_2}$ for some unknown scale factor λ, which is cumbersome (McGLONE et al. 2004). But this can be realized easily by testing the identity of their reduced coordinates as follows. (1) Spherically normalize the lines $\mathbf{L}_i^s = \mathbf{L}_i / |\mathbf{L}_i|$ and derive their 6×6-covariance matrix $\Sigma_{\mathbf{L}_i^s \mathbf{L}_i^s}$ by variance propagation similar to the normalization of 2D points in (8). The constraint to be tested now reads simply as $\mathbb{E}(\underline{\mathbf{L}}_2^s - \underline{\mathbf{L}}_1^s) = \mathbf{0}$. (2) Change to reduced coordinates, as the covariance matrix of the difference is singular. This requires the choice of an approximate 3D line $\mathbf{L}^a$, close to the given ones, approximating the mean μ_L and using $\underline{\mathbf{L}}_{ri} = J_r^T(\mathbf{L}^a) \underline{\mathbf{L}}_i$, see (21). We may choose one of both lines. The constraint with reduced coordinates now reads as

$$\mathbb{E}(\underline{\mathbf{L}}_{r2} - \underline{\mathbf{L}}_{r1}) = \mathbf{0}. \qquad (32)$$

In case the two lines are mutually statistically independent the optimal test statistic now is

$$\underline{T} = \underline{\mathbf{d}}^T \Sigma_{dd}^{-1} \underline{\mathbf{d}} \sim \chi_4^2, \qquad (33)$$

with the difference and its regular covariance matrix

$$\underline{\mathbf{d}} = \underline{\mathbf{L}}_{r2} - \underline{\mathbf{L}}_{r1}, \qquad (34)$$

$$\Sigma_{dd} = \Sigma_{L_{r1} L_{r1}} + \Sigma_{L_{r2} L_{r2}}. \qquad (35)$$

The test statistic $\underline{T}$ is χ_4^2-distributed in case the null-hypothesis, namely if the two lines are identical, holds. It obviously is the Mahalanobis distance of the two reduced line coordinates, thus can be used to measure the difference between two 3D lines.

The test on the identity of two entities using their minimal representation, thus their reduced coordinates can be applied to all geometric entities and also to all homogeneous transformations.

4 Example: Estimating 3D Line from Image Line Segments

The following example demonstrates the practical use of the proposed method: namely determining 3D lines from image line segments. Fig. 4 shows three images taken with a CANON 450D. The focal length was determined using vanishing points, the principal point was assumed to be the image centre, the images were not corrected for lens distortion. The images then were mutually oriented using a bundle adjustment program. Straight line segments were automatically detected and a small subset of 12, visible in all three and pointing in the three principal directions were manually brought into correspondence. From the straight lines l_{ij} ($\mathbf{l}'_{ij}$), $i = 1, …, 12$; $j = 1, 2, 3$ and the projection matrices P_j we determined the projection planes $\mathbf{A}_{ij} = \mathsf{P}_j^\mathsf{T} \mathbf{l}'_{ij}$ of the line segments. For determining the ML estimates of the 12 lines $\mathbf{L}_i$, each from the three corresponding projection planes, we needed their covariance matrices. They were determined by variance propagation based on the covariance matrices of the image lines $\mathbf{l}_{ij}$ and the covariance matrices of the projection matrices.

As we did not have the cross-covariance matrices between any two of the projection matrices, we only used the uncertainty $\Sigma_{Z_j Z_j}$ of the three projection centres Z_j. The covariance matrices of the straight line segments were derived from the uncertainty given by the feature extraction. For this we fitted a straight line through the edge pixels, which was assumed to be determinable with a standard deviation of $\sigma_p = 0.3$ pixel]. The covariance matrix of the projection planes then is determined by variance propagation of $\mathbf{A}_{ij} = \mathsf{P}_i^\mathsf{T} \mathbf{l}'_{ij} = (I_4 \otimes \mathbf{l}'_{ij}) \operatorname{vec} \mathsf{P}_j$ from $\Sigma_{\mathbf{A}_{ij} \mathbf{A}_{ij}} = \mathsf{P}_i^\mathsf{T} \Sigma_{\mathbf{l}'_i \mathbf{l}'_i} \mathsf{P}_i + (I_4 \otimes \mathbf{l}'_{ij}) \Sigma_{p_i p_i} (I_4 \otimes \mathbf{l}'^\mathsf{T}_{ij})$.

We achieved the following results. First, the square roots $\hat{\sigma}_0$ of the estimated variance factors $\hat{\sigma}_0^2 = \Omega/(G - U)$ range between 0.03 and 3.2. As the degrees of freedom for each 3D line estimation is $G - U = 2I - 4 = 2 \cdot 3 - 4 = 2$, thus in this case is very low, such a spread is to be expected. The mean value for the 12 variance factors is 1.1, which confirms the model to fit to the data.
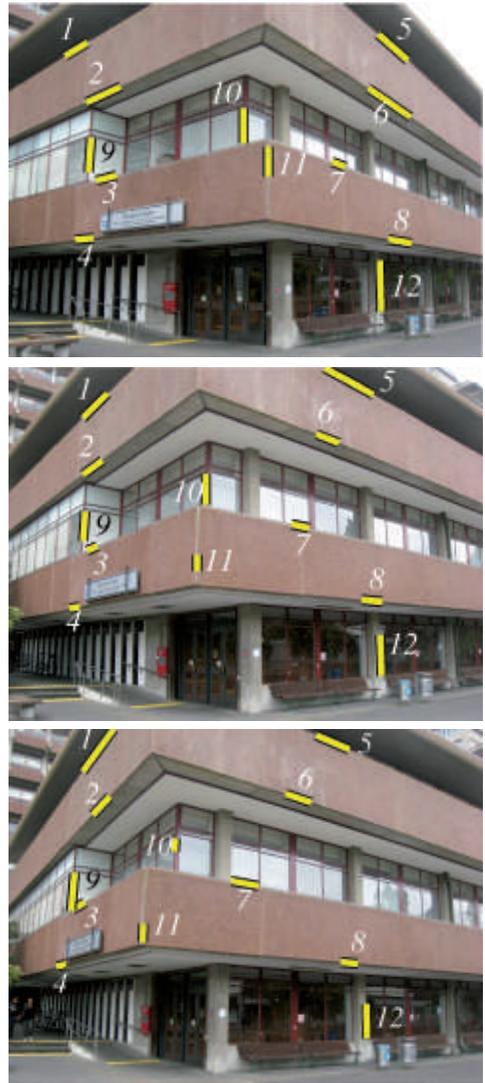
Fig. 4: Three images with 12 corresponding straight line segments used for the reconstruction of the 3D lines, forming three groups [1...4], [5...8], [9...12] for three main directions.

As a second result we analysed the angles between the directions of the 12 lines. As they are clustered into three groups corresponding to the main directions of the building, we should find values close to 0° within a group and values close to 90° between lines of different groups. The results are collected in Tab. 1.

The angles between lines in the same group scatter between 0° and 14.5°, the angles be-

Tab. 1: Result of determining 12 lines from the images in Fig. 4. Left column: minimal length l of the three line segments involved. Upper right triangle: angles between the lines. Lower left triangle: values of the test statistic for the deviation from 0° or 90°.

l_{min} \#	1	2	3	4	5	6	7	8	9	10	11	12
173 pixel	–	2.6°	2.7°	3.0°	88.6°	89.0°	88.7°	76.5°	86.7°	87.0°	86.6°	85.2°
155 pixel	0.7	–	0.7°	1.6°	89.9°	89.7°	87.3°	75.1°	89.0°	89.2°	88.9°	87.4°
72 pixel	0.7	0.	–	0.9°	89.4°	89.8°	87.9°	75.6°	89.4°	89.6°	89.3°	87.8°
62 pixel	1.2	0.3	0.1	–	88.5°	88.9°	88.7°	76.4°	89.8°	90.0°	89.7°	88.2°
232 pixel	0.6	0.0	0.1	0.2	–	0.4°	2.8°	15.3°	89.6°	89.3°	89.7°	89.1°
153 pixel	0.3	0.1	0.0	0.1	0.1	–	2.4°	14.9°	89.5°	89.2°	89.6°	89.1°
91 pixel	0.5	0.8	0.4	0.2	0.8	0.6	–	12.5°	89.0°	88.7°	89.1°	88.6°
113 pixel	1.0	1.1	1.1	0.9	1.1	1.1	0.8	–	87.0°	86.7°	87.2°	87.0°
190 pixel	1.6	0.4	0.3	0.1	0.2	0.3	1.0	1.3	–	0.4°	0.2°	1.6°
82 pixel	1.4	0.3	0.2	0.0	0.4	0.4	1.2	1.4	0.5	–	0.5°	1.8°
103 pixel	1.6	0.5	0.4	0.2	0.2	0.2	0.9	1.2	0.3	0.6	–	1.6°
225 pixel	2.4	1.1	1.1	1.0	0.5	0.5	1.3	1.5	3.2	3.6	4.0	–

tween lines of different orientation differ from 90° between 0° and 15°. The standard deviations of the angles scatter between 0.4° and 8.3°, this is why none of the deviations from 0 or 90° are significant.

The statistical analysis obviously makes the visual impression objective.

Further examples on the rigour and superiority of representation within vanishing point estimation and 3D line intersection are given in FÖRSTNER (2010 a,b).

5 Conclusions and Outlook

The paper proposes a minimal representation of uncertain homogeneous entities, vectors or matrices, useful for testing and estimation. It avoids the redundancy of the homogeneous representations. Therefore no additional constraints are required to enforce the normalization of the entities including the Plücker constraints for 3D lines. In addition we not only obtain a minimal representation for the uncertainty of the geometric elements, but also simple means to determine the Mahalanobis distance between two elements, which may be used for testing or for grouping. The covariance matrices of the minimal representation of observed entities are regular allowing a transparent definition of a maximum likelihood es-

timation. We demonstrated the rigour of the method with the estimation of 3D lines from projection planes in a multi-view setup.

The convergence properties when using the proposed reduced representation does not change as the solution steps are algebraically equivalent. The main advantage of the proposed concept is the ability to handle elements at or close to infinity and the full range of the transformations without loosing numerical stability and that the representation is minimal, which allows to use the representation for large estimation problems, such as the bundle adjustment. The concept can be extended to higher level algebras, such as the geometric or the conformal algebra (GEBKEN 2009) where the motivation to use minimal representations is even higher than in our context.

Acknowledgement

References

ÅSTROM, K. , 1998: Using Combinations of Points, Lines and Conics to Estimate Structure and Mo-

tion. – Proc. of Scandinavian Conference on Image Analysis.

BARTOLI, A. & STURM, P., 2004: Non Linear Estimation of the Fundamental Matrix With Minimal Parameters. – IEEE Transactions on Pattern Analysis and Machine Intelligence **26** (4): 426–432.

BARTOLI, A. & STURM, P., 2005: Structure-from-Motion Using Lines: Representation, Triangulation and Bundle Adjustment. – Computer Vision and Image Understanding **100:** 416–441.

BEGELFOR, E. & WERMAN, M., 2005: How to Put Probabilities on Homographies. – IEEE Trans. Pattern Anal. Mach. Intell. **27** (10): 1666–1670.

BREGLER, C. & MALIK, J., 1998: Tracking people with twists and exponential maps. – Conference on Computer Vision and Pattern Recognition. IEEE Computer Society, Los Alamitos, CA, USA, 8–15.

COLLINS, R., 1993: Model Acquisition Using Stochastic Projective Geometry, PhD thesis. – Department of Computer Science, University of Massachusetts: Also published as UMass Computer Science Technical Report TR95-70.

CRIMINISI, A. , 2001: Accurate Visual Metrology from Single and Multiple Uncalibrated Images. – Springer-Verlag London Ltd.

FÖRSTNER, W., 2010a: Minimal Representations for Uncertainty and Estimation in Projective Spaces. – Proc. of Asian Conference on Computer Vision.

FÖRSTNER, W., 2010b: Optimal Vanishing Point Detection and Rotation Estimation of Single Images of a Legolandscene. – Int. Archives of Photogrammetry and Remote Sensing. ISPRS Symposium Comm. III, Paris.

GEBKEN, C., 2009: Conformal Geometric Algebra in Stochastic Optimization. – PhD thesis, Christian-Albrechts-University of Kiel, Institute of Computer Science.

HARTLEY, R.I. & ZISSERMAN, A., 2000: Multiple View Geometry in Computer Vision. – Cambridge University Press.

HEUEL, S., 2004: Uncertain Projective Geometry: Statistical Reasoning for Polyhedral Object Reconstruction, Volume 3008 of LNCS. – Springer: PhD Thesis.

KANATANI, K., 1996: Statistical Optimization for Geometric Computation: Theory and Practice. – Elsevier Science.

McGLONE, J.C., MIKHAIL, E.M. & BETHEL, J.S., 2004: Manual of Photogrammetry. – Am. Soc. of Photogrammetry and Remote Sensing.

MEIDOW, J., 2011: Efficient video mosaicking by multiple loop closing. – Proc. of Photogrammetric Image Analysis: 1–12.

MEIDOW, J., BEDER, C. & FÖRSTNER, W., 2009: Reasoning with Uncertain Points, Straight Lines, and Straight Line Segments in 2D. – International Journal of Photogrammetry and Remote Sensing **64:** 125–139.

ROSENHAHN, B., GRANERT, O. & SOMMER, G., 2002: Monocular pose estimation of kinematic chains. – DORST, L., DORAN, C. & LASENBY, J. (eds.). – Applications of Geometric Algebra in Computer Science and Engineering. Proc. AGACSE 2001: 373–375, Cambridge, UK. Birkhäuser Boston.

SCHNEIDER, J., SCHINDLER, F. & FÖRSTNER, W., 2011: Bündelausgleichung für Multikamerasysteme. – Proceedings of the 31th DGPF Conference.

STURM, P. & GARGALLO, P., 2007: Conic fitting using the geometric distance. – Proceedings of the Asian Conference on Computer Vision **2:** 784–795, Springer, Tokyo, Japan.

Address of the Author:

Prof. Dr.-Ing. Dr. h.c. mult. WOLFGANG FÖRSTNER, Josef-Schell-Straße 34, 53121 Bonn, Germany, Tel.: +49-228-472223, e-mail: wf@ipb.uni-bonn.